Dynamics of a Random Vibration Excited Discrete Packaging System with Hyperbolic Tangent Nonlinearity

Songping Yang

Key Laboratory of Product Packaging and Logistics of Guangdong Higher Education Institutes, College of Packaging Engineering, Jinan University, Zhuhai 519070, China.
School of Mechanics and Construction Engineering, Jinan University, Guangzhou 510632, China.
E-mail: tysp@jnu.edu.cn

Peichang Deng

Key Laboratory of Product Packaging and Logistics of Guangdong Higher Education Institutes, College of Packaging Engineering, Jinan University, Zhuhai 519070, China.

(Received 15 November 2025; accepted 12 April 2026)

This paper presents a systematic investigation into the dynamical characteristics of a randomly excited multi-degree-of-freedom (MDOF) discrete product packaging system (DPPS) featuring hyperbolic tangent nonlinearity, with emphasis placed on an acceleration response analysis. Because the analytical solution of the acceleration response spectrum for the hyperbolic tangent DPPS has rarely been investigated, then the approximate analytical solution is established to predict the acceleration response of the Gaussian vibration excited system. Secondly, Hermite polynomial is adopted to simulate non-Gaussian vibration excitation, and verified by the actual road excitation signal. On this basis, the non-Gaussian random vibration analysis method is introduced to analyze the acceleration response of the system, the sensitivity of the response is discussed. Then, the failure analysis for the desktop computer package via the first-passage failure probability of the acceleration response is given. The approximate analytical solution can effectively predict the acceleration response of the Gaussian random vibration excited system. The proposed non-Gaussian vibration analysis approach can conveniently reproduce actual non-Gaussian vibration excitation and analyze the dynamic properties. Since the "soft spring" effect of hyperbolic tangent cushion material, there exists an optimal nonlinear parameter β^*, which can minimize the acceleration response of critical components. The failure mechanism of critical components in a desktop computer package subjected to non-Gaussian vibration is elucidated, and a reliability analysis is presented based on a predetermined product fragility. Moreover, an appropriate cushioning design can be determined for a specified reliability level. This study offers guidance for the vibration absorption design of packaging systems.

1. INTRODUCTION

Vibration constitutes the primary cause of product failure in logistics environments.[1] To effectively evaluate the protective performance of packaging, mature packaging products are required to undergo vibration reliability tests. In accordance with the principle of accelerated vibration, Gaussian vibration excitation is generally adopted in such tests[1–3] Gaussian random vibration is a classical model employed in the laboratory reliability assessment of product packaging, widely used to analyze the dynamic response characteristics of packaging structures. However, most vibration excitations encountered in actual logistics environments exhibit non-Gaussian distribution characteristics[5–7] many products that successfully pass the Gaussian vibration reliability test still suffer from damage under non-Gaussian vibration excitations in actual logistics scenarios.

Vibration excitations from different countries have been collected to characterize the vibration environments for product packaging.[8–11] To accurately reproduce actual vibration signals in laboratory tests, various state-of-the-art laboratory reproduction methods have been developed.[12,13] These studies are valuable for the design and validation of product and packaging systems during transportation. The spring-mass-damper model was first adopted by Mindlin[14] to represent product packaging systems. Considering the nonlinear constitutive behavior of cushioning packaging materials,[15] classical packaging systems with cubic, tangent, and hyperbolic tangent stiffness have been introduced to investigate the dynamic protection performance of product packaging.[16,17] Since the force-deformation relationships of many cushioning materials, such as preloaded expandable polystyrene (EPS) foam and neoprene, exhibit a hyperbolic tangent elastic property[18,19] the damage boundary theory for hyperbolic tangent packaging systems has been further explored based on impact theory.[20–22] Although the dynamics of hyperbolic tangent packaging systems under shock excitation have been systematically investigated,[23,24] such excitation is typically described by a deterministic function.

However, the actual logistics process involves various uncertainties, and product packaging damage frequently occurs due to random vibration. Therefore, stochastic problems related to packaging systems have attracted increasing attention from researchers.[25] Thakur et al.[26] introduced a piecewise nonlinear model for a single-degree-of-freedom (SDOF) pack-

aging system and derived the displacement response under random vibration. Gan[27] investigated a SDOF cubic nonlinear packaging system under Gaussian white noise excitation, and analyzed the displacement responses of the system under both non-resonant and resonant conditions. Zhu[28,29] studied the vibration reliability of a SDOF cubic nonlinear packaging system considering a critical component under Gaussian random vibration. Subsequently, a methodology was proposed to achieve accurate simulation of non-Gaussian excitation and efficient analysis of the time-dependent reliability of the packaging system. The above studies mainly focus on the random vibration analysis of SDOF systems, with the main consideration being the nonlinearity, including linearity, piecewise linearitt,[30] and piecewise nonlinearity[31] caused by packaging materials. However, few investigations have been conducted on the stochastic vibration dynamics of hyperbolic tangent packaging systems. Nevertheless, damage to hyperbolic tangent product packaging caused by random vibrations during actual logistics is frequently observed, which has attracted attention to the stochastic problem of hyperbolic tangent packaging.[32] In a prior study, Yang[33] drived the approximate analytical solution for the power spectrum of the acceleration responses of a SDOF hyperbolic tangent packaging system. Furthermore, a new numerical method was proposed to perform non-Gaussian random vibration analysis of a two-degree-of-freedom (TDOF) hyperbolic tangent packaging system.[34] The analytical solution for the acceleration response spectrum of the TDOF system has not yet been obtained. Since a product typically contains more than one critical component,[35] product packaging considering multiple critical components has been modeled as a general MDOF DPPS model for the dynamics analysis.

It is a noteworthy finding that MDOF DPPS is very similar to the multiple tuned mass damper (MTMD), which was firstly proposed by Clark.[36] MTMD, the most popular passive control device, was widely used to control the vibration of the primary system in engineering vibration because of its advantages of simple structure and good stability. H_2, H_∞ methods[37,38] were proposed to establish the objective function using as optimization analysis of vibration reduction. On that basis, the gradient-based root-mean-square response minimization was proposed and proved to be equally effective.[39] It is common to consider the case where the primary system is linear, and the effect of MTMD on nonlinear structures was studied through the energy theory.[40] The nonlinearity[41] was added to a traditional linear vibration reduction device in order to effectively increase the vibration suppression bandwidth and improve the robustness of the vibration reduction system. Hence, the primary system coupled with a nonlinear energy sink (NES) under a narrow-band random excitation was investigated.[42] A detailed response regimes of linear oscillator attached NES under harmonic external forcing was analyzed, and the possible application of the NES for vibration absorption and mitigation was also evaluated.[43] The NES was introduced as its restoring force was tailored according to the nonlinear restoring force of the primary system.[44] And some new MTMD such as the tunable flexure's vibration absorbers,[45] multi active tuned mass dampers,[46] tuned viscous mass dampers,[47] tuned mass dampers paired with elastomeric bearings[48] and so on were introduced, the optimal parameters of MTMD for control performance and energy dissipation were discussed in detail.[49–51] However, it is not difficult to find that the hyperbolic tangent nonlinearity is rarely considered in the nonlinear primary system, and MTMD and NES usually optimized vibration reduction of the primary system or structure.[52] Now it's just the other way around, the product packaging optimization design is using the cushion packaging system (mean. primary system) to optimized vibration reduction of the critical component systems (mean. MTMD or NES).

On the one hand, several standards currently exist for implementing laboratory testing regimes suitable for road transport packaging. Although these protocols based on Gaussian vibration are still functioning effectively, they are more often regarded as a compromise between economy, cost, and reliability.[53] On the other hand, non-Gaussian reliability analysis methods are being developed in full swing,[54] aiming to overcome the limitations of laboratory-simulated Gaussian vibration and further develop non-Gaussian vibration specifications for transport packaging. Transport environment excitation is characterized by the acceleration road spectrum, which serves as a key index for reliability assessment.[55,56] Therefore, the study of acceleration responses is particularly significant for evaluating the reliability design of product packaging.[57] Since the analytical solution of acceleration response spectrum of hyperbolic tangent MDOF DPPS has rarely been investigated. A more systematic random vibration analysis of the hyperbolic tangent nonlinear MDOF DPPS is carried out. Therefore, this paper focuses on the dynamical properties of MDOF DPPS considering multiple critical components under Gaussian and non-Gaussian random vibration, meanwhile explores the mechanism of the cushion packaging primary system as well as the coupling effects between critical components.

The rest of this paper is organized as follows: In Section 2, the packaged product with multiple critical components is modeled as a general model of MDOF DPPS, and the system dynamic equation is given. An approximate analytical solution is established to predict the acceleration response spectrum of the hyperbolic tangent MDOF DPPS under Gaussian random vibration, and verified by the numerical solution of $3+1$ DOF DPPS in Section 3. In Section 4, the non-Gaussian random vibration analysis method is introduced, then the reliability analysis for the desktop computer package is given. In Section 5, the conclusions are presented in the final section of the paper.

2. MODELLING AND FORMULATION

Throughout the logistics process, the product is subjected to external excitations. Due to the superimposed structural configuration between the critical components and the product main body, these components often exhibit a greater dynamic response. Moreover, the fragility of critical components is typically lower than that of the product body, making them more susceptible to damage and consequently leading to functional failure of the product. The product packaging system is a MDOF system comprising multiple critical components coupled with the product body via connectors. Therefore, to enable further investigation and optimization, it is essential to establish a generalized model that can analyze and elucidate the underlying interaction mechanisms among all product components.

2.1. Discrete Product Packaging Modelling

Taking a packaged desktop computer as an example, the system is consisted of a computer host and n critical components, such as the hard disk, motherboard, and others. Employing the lumped mass method, the packaged computer incorporating multiple critical components is conceptualized as a generalized $i+1$ DOF DPPS, as depicted in Fig. 1.

In Fig. 1, m_p, m_i represent the mass of the computer host and ith critical components, respectively. $F(\delta)$, c_p are the stiffness and damping of the cushion packaging material, respectively. k_i, c_i denote the stiffness and damping of the connected system between the ith critical component and the computer host, respectively. $y(t)$ is the external displacement excitation, $x_p(t)$, $x_i(t)$ respectively signify the displacement of product body and the ith critical component.

Thus, the governing equations of motion for the system subjected to a prescribed base displacement excitation can be formulated as follows:

$$\begin{cases} m_p\ddot{x}_p = -c_p(\dot{x}_p-\dot{y}) + \sum_{i=1}^{n} c_i(\dot{x}_i-\dot{x}_p) - \\ \qquad F(x_p-y) + \sum_{i=1}^{n} k_i(x_i-x_p); \\ m_i\ddot{x}_i = -c_i(\dot{x}_i-\dot{x}_p) - k_i(x_i-x_p). \end{cases} \tag{1}$$

Introducing the following relative displacement:

$$\begin{cases} \delta_p = x_p - y; \\ \delta_i = x_i - x_p; \end{cases} \qquad (i=1,2,\ldots,n); \tag{2}$$

Eq. (1) can be rewritten in terms of relative displacement:

$$\begin{cases} m_p\ddot{\delta}_p + c_p\dot{\delta}_p - \sum_{i=1}^{n} c_i\dot{\delta}_i + F(\delta_p) - \sum_{i=1}^{n} k_i\delta_i = -m_p\ddot{y}; \\ m_i\ddot{\delta}_i + m_i\ddot{\delta}_i + c_i\dot{\delta}_i + k_i\delta_i = -m_i\ddot{y}; \end{cases} \\ (i=1,2,\ldots,n). \tag{3}$$

By introducing the following notations:

$$\begin{cases} \frac{k_p}{m_p} = \omega_p^2, \quad \frac{k_i}{m_i} = \omega_i^2, \quad \frac{m_i}{m_p} = a_i, \\ \frac{c_p}{\sqrt{k_p m_p}} = 2\xi_p, \quad \frac{c_i}{\sqrt{k_i m_i}} = 2\xi_i; \end{cases} \tag{4}$$

Eq. (3) can be rewritten:

$$\begin{cases} \ddot{\delta}_p + 2\xi_p\omega_p\dot{\delta}_p - \sum_{i=1}^{n} 2a_i\xi_i\omega_i\dot{\delta}_i + \frac{F(\delta_p)}{m_p} - \\ \qquad \sum_{i=1}^{n} a_i\omega_i^2\delta_i = w(t); \\ \ddot{\delta}_i + 2\xi_i\omega_i\dot{\delta}_i + \omega_i^2\delta_i - 2\xi_p\omega_p\dot{\delta}_p + \sum_{i=1}^{n} 2a_i\xi_i\omega_i\dot{\delta}_i - \\ \qquad \frac{F(\delta_p)}{m_p} + \sum_{i=1}^{n} a_i\omega_i^2\delta_i = 0; \end{cases} \\ (i=1,2,\ldots,n); \tag{5}$$

where $w(t)$ denotes the base acceleration excitation $-\ddot{y}$ which is assumed to be a stationary zero-mean white Gaussian noise with spectral density K, k_p represents the stiffness of the initial linear elastic stage of the cushion packaging material. Further simplifying, the acceleration response of the computer host and ith critical component can be solved by the Eq. (6):

$$\begin{cases} m_p\ddot{x}_p = -c_p\dot{\delta}_p + \sum_{i=1}^{n} c_i\dot{\delta}_i - F(\delta_p) + \sum_{i=1}^{n} k_i\delta_i; \\ m_i\ddot{x}_i = -c_i\dot{\delta}_i - k_i\delta_i; \end{cases} \\ (i=1,2,\ldots,n); \tag{6}$$

as $F(\delta_p) = k_p\delta_p$, the system is simplified as a linear MDOF DPPS.

2.2. Hyperbolic Tangent Discrete Product Packaging

It has been reported[27,28] that the relationship between the nonlinear restoring force $F(\delta)$ and the deformation δ for many cushion packaging materials (e.g., polyurethane foam and neoprene) follows a hyperbolic tangent type elastic property, as depicted in Fig. 2.

It can be seen from Fig. 2a the compression test result of the polyurethane foam follows the hyperbolic tangent relation shown in Fig. 2b, which can be described by the Eq. (7):

$$F(\delta_p) = F_0 \tanh\left(\frac{k_p}{F_0}\delta_p\right) = F_0\tanh(\beta\delta_p); \tag{7}$$

where k_p is the initial linear elastic coefficient of the hyperbolic tangent cushion material, F_0 denotes the restoring force limit of the cushion material, β which is defined as the ratio of the initial elastic modulus k_p to the restoring force limit F_0, represents the system nonlinear characteristic parameter of the hyperbolic tangent cushion material. A higher initial elastic modulus combined with a lower restoring force limit results in a steeper $F-\delta$ curve and stronger nonlinearity. This characteristic enables such materials to maintain a nearly constant force on the product over a wide range of deformation, even under heavy external loads, thereby offering enhanced protection.

Then, the dynamic equation of hyperbolic tangent MDOF DPPS can be written:

$$\begin{cases} \ddot{\delta}_p + 2\xi_p\omega_p\dot{\delta}_p - \sum_{i=1}^{n} 2a_i\xi_i\omega_i\dot{\delta}_i + \frac{\omega_p^2}{\beta}\tanh(\beta\delta_p) - \\ \qquad \sum_{i=1}^{n} a_i\omega_i^2\delta_i = w(t); \\ \ddot{\delta}_i + 2\xi_i\omega_i\dot{\delta}_i + \omega_i^2\delta_i - 2\xi_p\omega_p\dot{\delta}_p + \sum_{i=1}^{n} 2a_i\xi_i\omega_i\dot{\delta}_i - \\ \qquad \frac{\omega_p^2}{\beta}\tanh(\beta\delta_p) + \sum_{i=1}^{n} a_i\omega_i^2\delta_i = 0; \end{cases} \\ (i=1,2,\ldots,n). \tag{8}$$

3. ACCELERATION RESPONSE SPECTRUM OF THE GAUSSIAN VIBRATION EXCITED SYSTEM

Gaussian random vibration, a classic model for analyzing packaging structure and basic dynamic response characteristics, is commonly employed in laboratory reliability assessments of product packaging. Within this context, acceleration response analysis is particularly crucial for evaluating the reliability design of packaging systems. However, to the best of the authors' knowledge, the approximate analytical solution for the acceleration response spectrum of a hyperbolic tangent DPPS under random excitation has yet to be investigated.

3.1. Approximate Analytical Solution

The approximate analytical solution for the acceleration response spectrum of the hyperbolic tangent MDOF DPPS is derived through the following steps:

(1) The dynamic Eq. (8) of the system is replaced by the following equivalent linear system:

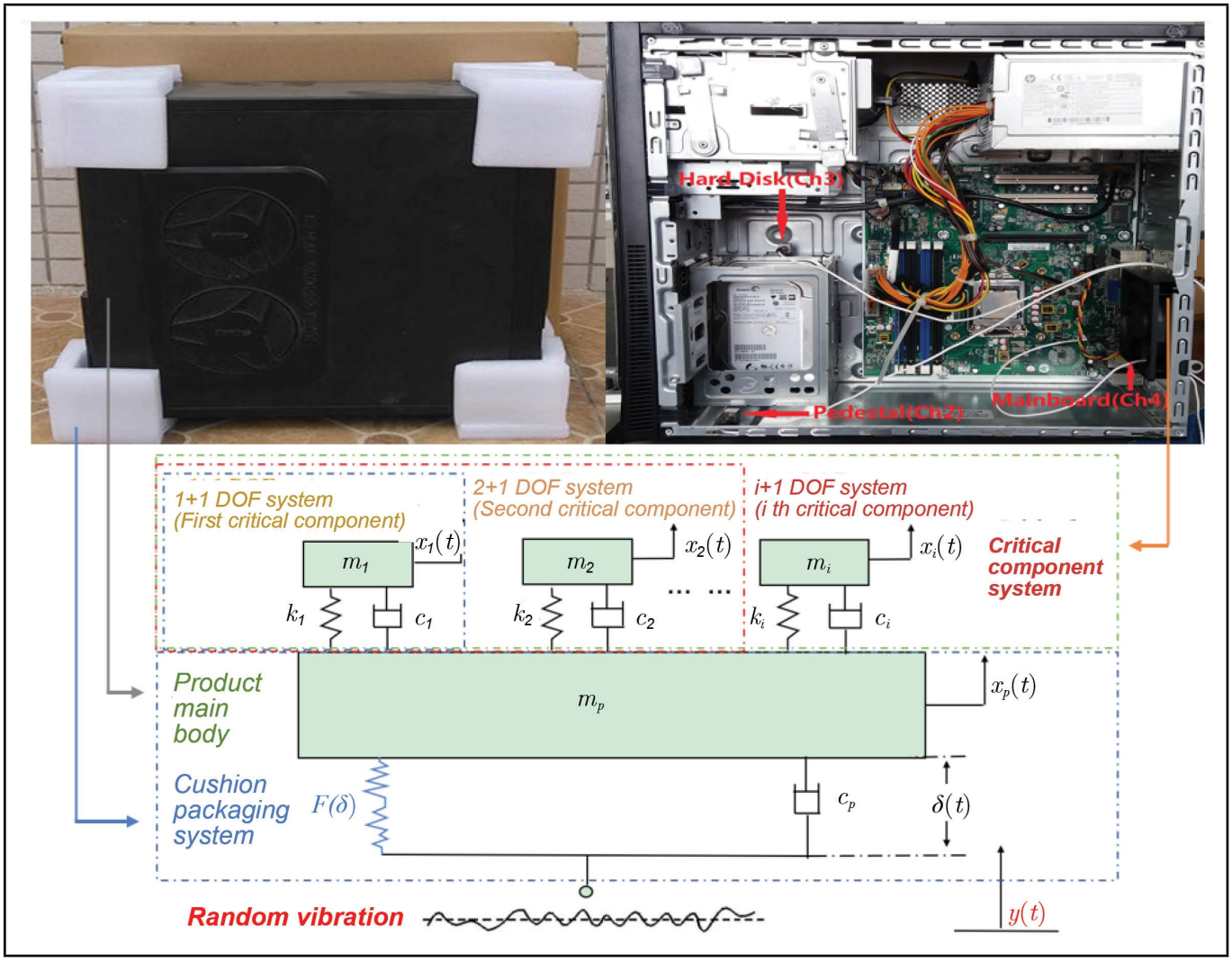

Figure 1. A general model of $i+1$ DOF nonlinear DPPS for packaged desktop computer.

$$\begin{cases} \ddot{\delta}_p + 2\xi_p\omega_p\dot{\delta}_p - \sum_{i=1}^{n} 2a_i\xi_i\omega_i\dot{\delta}_i + a_e\omega_p^2\delta_p - \\ \qquad \sum_{i=1}^{n} a_i\omega_i^2\delta_i = w(t), \\ \ddot{\delta}_i + 2\xi_i\omega_i\dot{\delta}_i + \omega_i^2\delta_i - 2\xi_p\omega_p\dot{\delta}_p + \sum_{i=1}^{n} 2a_i\xi_i\omega_i\dot{\delta}_i - \\ \qquad a_e\omega_p^2\delta_p + \sum_{i=1}^{n} a_i\omega_i^2\delta_i = 0; \end{cases} \quad (i = 1, 2, \ldots, n); \tag{9}$$

where a_e is the equivalent stiffness coefficient.

According to the principle of minimum difference between the equivalent system and the original system,[2] it can be defined:

$$a_e = \frac{E[\delta_p(\frac{\omega_p^2}{\beta}\tanh(\beta\delta_p))]}{E[\delta_p^2]}. \tag{10}$$

Expand the hyperbolic tangent function using the Taylor series formula:

$$\tanh(\beta\delta_p) = \beta\delta_p - \frac{(\beta\delta_p)^3}{3} + \frac{2(\beta\delta_p)^5}{15} - \frac{17(\beta\delta_p)^7}{315}. \tag{11}$$

It can be seen from the Eq. (11) that as $\beta\delta_p \gg \frac{(\beta\delta_p)^3}{3}$ i.e.$(\beta\delta_p)^2 \ll 1$, the system can be regarded as a linear system. Combining with Eq. (10) and ignoring infinitesimals of the sixth order and higher, the equivalent stiffness coefficient a_e can be expressed:

$$a_e = \frac{E\left[\delta_p^2\right] - E\left[\beta\delta_p^4\right]}{E[\delta_p^2]} = 1 - \frac{\beta^2 m_{4000}}{3m_{2000}}. \tag{12}$$

Here, m_{4000} and m_{2000} are the fourth order cumulant and the second order cumulant, respectively. From Eq. (12), it can be seen that the range of equivalent linearization is affected by $\frac{\beta^2 m_{4000}}{3m_{2000}}$.

(2) Let $X_1 = \delta_p$, $X_2 = \dot{\delta}_p$, $X_i = \delta_i$, $X_{i+1} = \dot{\delta}_{i+1}$, where $(i = 1, 2, \ldots, n)$, the Ito equation[59] can be obtained:

$$\begin{cases} dX_1 = X_2 dt; \\ dX_2 = (-2\xi_p\omega_p X_2 + \sum_{i=1}^{n} 2a_i\xi_i\omega_i X_{i+1} + \\ \qquad \sum_{i=1}^{n} a_i\omega_i^2 X_i - a_e\omega_p^2 X_1)\, dt + \sqrt{2\pi K}dB(t); \\ dX_i = X_{i+1}dt; \\ dX_{i+1} = [-\sum_{i=1}^{n}(1+2a_i)\xi_i\omega_i X_{i+1} - \\ \qquad \sum_{i=1}^{n}(1+a_i)\omega_i^2 X_i + 2\xi_p\omega_p X_2 + a_e\omega_p^2 X_1]\, dt; \end{cases} \tag{13}$$

where K denotes the spectral density of the white Gaussian noise with $w(t)$, $B(t)$ represents Wiener process, with the relationship given by $\frac{dB(t)}{dt} = w(t)$.

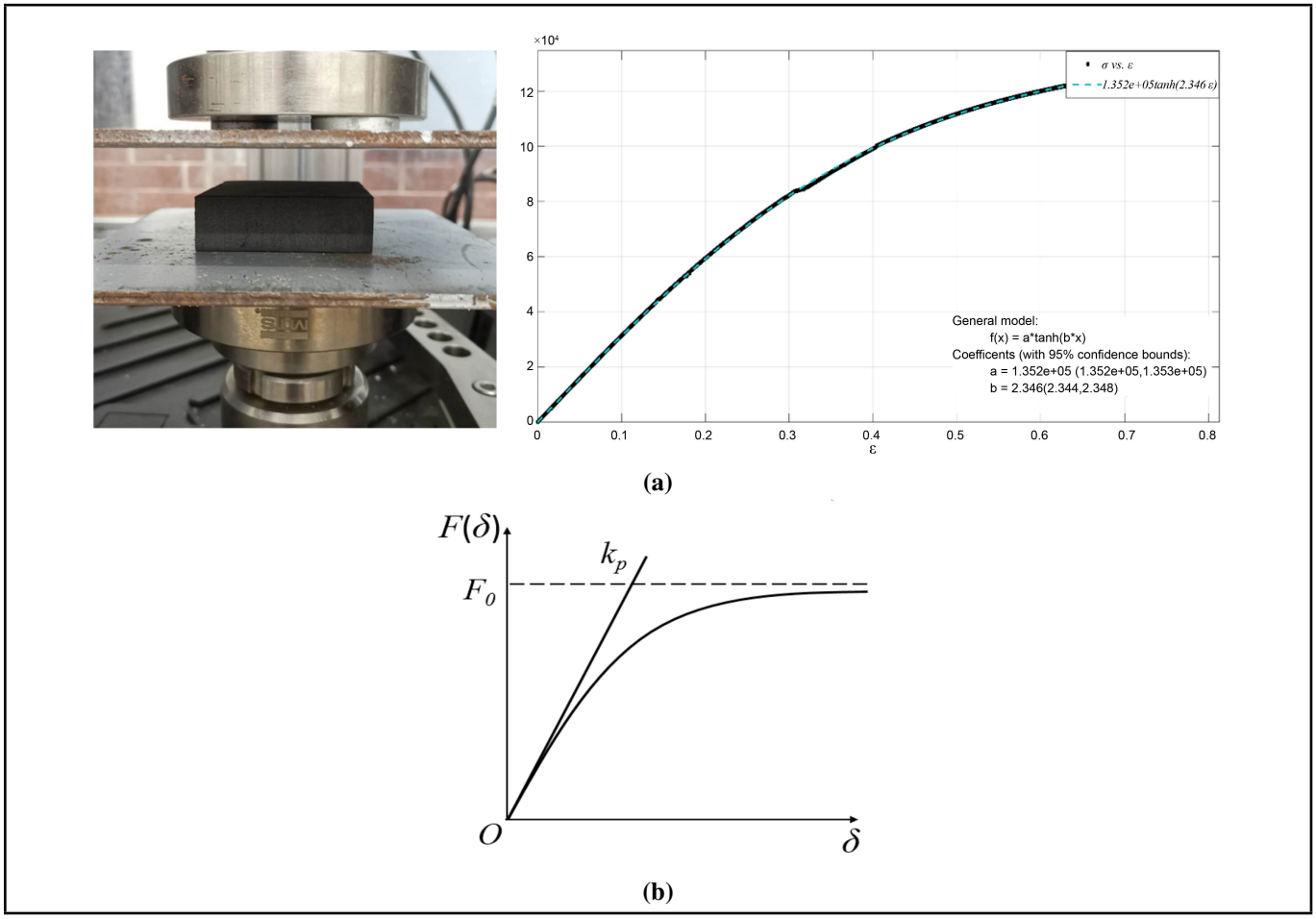

Figure 2. Elastic characteristic curve of hyperbolic tangent polyurethane foam. (a) Compression test result of the polyurethane foam; (b) Hyperbolic tangent type of elastic curve.

Multiplying both sides by $X_1(t)$ and $X_3(t)$, and taking the set average, Eq. (13) can be transformed into:

$$\begin{cases} \dfrac{dR_{11}(\tau)}{d\tau} = R_{12}(\tau); \\ \dfrac{dR_{12}(\tau)}{d\tau} = -2\xi_p\omega_p R_{12}(\tau) + \sum_{i=1}^{n} 2a_i\xi_i\omega_i R_{1,i+1}(\tau) \\ \quad - a_e\omega_p^2 R_{11}(\tau) + \sum_{i=1}^{n} a_i\omega_i^2 R_{1i}(\tau); \\ \dfrac{dR_{1i}(\tau)}{d\tau} = R_{1,i+1}(\tau); \\ \dfrac{dR_{1,i+1}(\tau)}{d\tau} = -\sum_{i=1}^{n}(1+2a_i)\xi_i\omega_i R_{1,i+1}(\tau) \\ \quad + 2\xi_p\omega_p R_{12}(\tau) + a_e\omega_p^2 R_{11}(\tau) \\ \quad - \sum_{i=1}^{n}(1+a_i)\omega_i^2 R_{1i}(\tau); \end{cases} \tag{14}$$

where $R_{ij}(\tau) = E(X_i(t)X_j(t))$ denotes the correlation between two variables $X_i(t)$ and $X_j(t)$, $(i, j = 1, 2, 3, 4)$.

$$\begin{cases} \dfrac{dR_{1i}(\tau)}{d\tau} = R_{2i}(\tau); \\ \dfrac{dR_{2i}(\tau)}{d\tau} = -2\xi_p\omega_p R_{2i}(\tau) + \sum_{i=1}^{n} 2a_i\xi_i\omega_i R_{i,i+1}(\tau) \\ \quad - a_e\omega_p^2 R_{1i}(\tau) + \sum_{i=1}^{n} a_i\omega_i^2 R_{ii}(\tau); \\ \dfrac{dR_{ii}(\tau)}{d\tau} = R_{i,i+1}(\tau); \\ \dfrac{dR_{i,i+1}(\tau)}{d\tau} = -\sum_{i=1}^{n}(1+2a_i)\xi_i\omega_i R_{i,i+1}(\tau) \\ \quad + 2\xi_p\omega_p R_{2i}(\tau) + a_e\omega_p^2 R_{1i}(\tau) \\ \quad - \sum_{i=1}^{n}(1+a_i)\omega_i^2 R_{ii}(\tau). \end{cases} \tag{15}$$

(3) According to the rules of integral transformation, Eq. (14) and Eq. (15) can be transformed into a frequency domain equation, respectively:

$$\begin{cases} i\omega\Phi_{11}(\omega) - \frac{1}{\pi}m_{2000} = \Phi_{12}(\omega); \\ i\omega\Phi_{12}(\omega) - \frac{1}{\pi}m_{1100} = -2\xi_p\omega_p\Phi_{12}(\omega) \\ \quad + \sum_{i=1}^{n} 2a_i\xi_i\omega_i\Phi_{1,i+1}(\omega) - a_e\omega_p^2\Phi_{11}(\omega) \\ \quad + \sum_{i=1}^{n} a_i\omega_i^2\Phi_{1i}(\omega); \\ i\omega\Phi_{1i}(\omega) - \frac{1}{\pi}m_{1010} = \Phi_{1,i+1}(\omega); \\ i\omega\Phi_{1,i+1}(\omega) - \frac{1}{\pi}m_{1001} = \\ \quad - \sum_{i=1}^{n}(1+2a_i)\xi_i\omega_i\Phi_{1,i+1}(\omega) + 2\xi_p\omega_p\Phi_{12}(\omega) \\ \quad + a_e\omega_p^2\Phi_{11}(\omega) - \sum_{i=1}^{n}(1+a_i)\omega_i^2\Phi_{1i}(\omega); \end{cases} \tag{16}$$

$$\begin{cases} i\omega\Phi_{1i}(\omega) - \frac{1}{\pi}m_{1010} = \Phi_{2i}(\omega); \\ i\omega\Phi_{2i}(\omega) - \frac{1}{\pi}m_{0110} = -2\xi_p\omega_p\Phi_{2i}(\omega) \\ \quad + \sum_{i=1}^{n} 2a_i\xi_i\omega_i\Phi_{1,i+1}(\omega) - a_e\omega_p^2\Phi_{1i}(\omega) \\ \quad + \sum_{i=1}^{n} a_i\omega_i^2\Phi_{ii}(\omega); \\ i\omega\Phi_{ii}(\omega) - \frac{1}{\pi}m_{0020} = \Phi_{i,i+1}(\omega); \\ i\omega\Phi_{i,i+1}(\omega) - \frac{1}{\pi}m_{0011} = \\ \quad - \sum_{i=1}^{n}(1+2a_i)\xi_i\omega_i\Phi_{i,i+1}(\omega) + 2\xi_p\omega_p\Phi_{2,i+1}(\omega) \\ \quad + a_e\omega_p^2\Phi_{1,i+1}(\omega) - \sum_{i=1}^{n}(1+a_i)\omega_i^2\Phi_{ii}(\omega); \end{cases} \tag{17}$$

where $m_{ijkl} = E[{X_1}^i {X_2}^j {X_i}^k {X_{i+1}}^l]$ can be obtained from Eq. (13).

By solving the above Eq. (14) and (15), $\Phi_{11}(\omega)$ and

$\Phi_{ii}(\omega)$ will be obtained, and then the acceleration response spectrum can be expressed with the real function. After simplifying the real part function and assigning the parameters except the parameter ω, the approximate analytical solution of acceleration power spectrum $\Phi_{\ddot{\delta}_p\ddot{\delta}_p}(\omega)$ and $\Phi_{\ddot{\delta}_i\ddot{\delta}_i}(\omega)$ can be given. Given the complexity and large number of equations involved in the MDOF system, the approximate analytical solution for the acceleration response spectrum of the hyperbolic tangent MDOF DPPS is efficiently obtained by implementing the above procedure in Mathematica software programming.

3.2. Numerical Verification

Taking the $3+1$ DOF DPPS as an example, namely, considering the system has three critical components and the product body unit, to verify the approximate analytical solution theory.

Dynamic equation can be written:

$$\begin{cases} \ddot{\delta}_p + 2\xi_p\omega_p\dot{\delta}_p - 2a_1\xi_1\omega_1\dot{\delta}_1 - 2a_2\xi_2\omega_2\dot{\delta}_2 - 2a_3\xi_3\omega_3\dot{\delta}_3 + \\ \quad \frac{\omega_p'^2}{\beta'}\tanh(\beta\delta_p) - a_1\omega_1^2\delta_1 - a_2\omega_2^2\delta_2 - a_3\omega_3^2\delta_3 = w(t); \\ \ddot{\delta}_1 + 2\xi_1\omega_1\dot{\delta}_1 + \omega_1^2\delta_1 - 2\xi_p\omega_p\dot{\delta}_p + 2a_1\xi_1\omega_1\dot{\delta}_1 + \\ \quad 2a_2\xi_2\omega_2\dot{\delta}_2 + 2a_3\xi_3\omega_3\dot{\delta}_3 - \frac{\omega_p^2}{\beta}\tanh(\beta\delta_p) + a_1\omega_1^2\delta_1 + \\ \quad a_2\omega_2^2\delta_2 + a_3\omega_3^2\delta_3 = 0; \\ \ddot{\delta}_2 + 2\xi_2\omega_2\dot{\delta}_2 + \omega_2^2\delta_2 - 2\xi_p\omega_p\dot{\delta}_p + \\ \quad 2a_1\xi_1\omega_1\dot{\delta}_1 + 2a_2\xi_2\omega_2\dot{\delta}_2 + 2a_3\xi_3\omega_3\dot{\delta}_3 - \frac{\omega_p^2}{\beta}\tanh(\beta\delta_p) \\ \quad + a_1\omega_1^2\delta_1 + a_2\omega_2^2\delta_2 + a_3\omega_3^2\delta_3 = 0; \\ \ddot{\delta}_3 + 2\xi_3\omega_3\dot{\delta}_3 + \omega_3^2\delta_3 - 2\xi_p\omega_p\dot{\delta}_p + 2a_1\xi_1\omega_1\dot{\delta}_1 + \\ \quad 2a_2\xi_2\omega_2\dot{\delta}_2 + 2a_3\xi_3\omega_3\dot{\delta}_3 - \frac{\omega_p^2}{\beta}\tanh(\beta\delta_p) + a_1\omega_1^2\delta_1 + \\ \quad a_2\omega_2^2\delta_2 + a_3\omega_3^2\delta_3 = 0. \end{cases} \tag{18}$$

The acceleration response of the product body and the ith critical component can be solved by the following formula:

$$\begin{cases} \ddot{x}_p = -2\xi_p\omega_p\dot{\delta}_p + 2a_1\xi_1\omega_1\dot{\delta}_1 + 2a_2\xi_2\omega_2\dot{\delta}_2 + \\ \quad 2a_3\xi_3\omega_3\dot{\delta}_3 - \frac{\omega_p^2}{\beta}\tanh(\beta\delta_p) + a_1\omega_1^2\delta_1 + a_2\omega_2^2\delta_2 + \\ \quad a_3\omega_3^2\delta_3; \\ \ddot{x}_1 = -\omega_1^2\delta_1 - 2\xi_1\omega_1\dot{\delta}_1; \\ \ddot{x}_2 = -\omega_2^2\delta_2 - 2\xi_2\omega_2\dot{\delta}_2; \\ \ddot{x}_3 = -\omega_3^2\delta_3 - 2\xi_3\omega_3\dot{\delta}_3. \end{cases} \tag{19}$$

Next, assuming the system parameters $\omega_p = 63$, $\omega_1 = 125, \omega_2 = 188, \omega_3 = 251, a_i = 0.01, \xi_p = 0.1, \xi_i = 0.01$, and conducting the Gaussian vibration excitation as $\mu = 0$, $\sigma^2 = 1$, $S = 0$, $K = 3$, the acceleration response theoretical spectrum of the $3+1$ DOF DPPS is obtained by Mathematica tool programming according to the steps introduced in Section 3.1.

Numerical verification is then conducted in MATLAB according to the following procedure:

Step 1: Generation of Gaussian excitation. The excitation signal is simulated using the *normrnd* function, which generates normally distributed random numbers. The signal parameters are set as follows: duration = 1000 s, time step = 0.001 s. These settings ensure a sufficiently large number of time-domain samples for accurate power spectral density (PSD) estimation.

Step 2: Initial condition setup. To replicate actual logistics conditions where the system starts from rest, the initial conditions for the $3+1$ DOF DPPS are set to zero: $\delta_p(0) = 0$, $\dot{\delta}_p = (0)$; $\delta_i(0) = 0$, $\dot{\delta}_i = (0)$, $(i = 1, 2, 3)$.

Step 3: Response computation and PSD analysis. The acceleration responses are computed via the fourth-order Runge-Kutta algorithm applied to Eq. (19). Subsequently, Welch's method is employed to estimate the PSD of these responses, using a Hanning window of 4096 points, a 75% overlap (3072 points), and a frequency resolution of $2\pi/dt$.

Step 4: Result comparison. The numerical PSD solutions for the three critical components and the main body are presented and validated against the theoretical solutions, as shown in Fig. 3.

As can be seen from Fig. 3, the numerical acceleration power spectra of each product component are in good agreement with their theoretical counterparts, which further validates the correctness of both the analytical and numerical models.

3.3. Method Applicability

Analysis of Eq. (11) reveals that the accuracy of the proposed method improves under the condition $\beta\delta_p \gg \frac{(\beta\delta_p)^3}{3}$ i.e. $(\beta\delta_p)^2 \ll 1$. This condition is readily satisfied in product package vibration testing, where the excitation is characterized by a low-magnitude acceleration PSD, leading to small δ_p responses. Moreover, the method remains valid for small values of the nonlinear characteristic parameter β of the hyperbolic tangent packaging materials, when system nonlinearity is weak. This is quantitatively expressed in Eq. (12) through the equivalent parameter $a_e = 1 - \frac{\beta^2 m_{4000}}{3m_{2000}}$ i.e. $\beta^2 m_{4000} \ll 3m_{2000}$, the method provides sufficient accuracy.

4. ACCELERATION RESPONSE ANALYSIS FOR THE NON-GAUSSIAN VIBRATION EXCITED SYSTEM

An acceleration response analysis method is established for the non-Gaussian random vibration of a hyperbolic tangent-type MDOF DPPS. Specifically, the Hermite polynomial method is employed to simulate non-Gaussian vibration excitation with specified mean, variance, skewness, and kurtosis, and its effectiveness is validated through comparison with actual road excitation signals. The acceleration response of the system under non-Gaussian excitation is subsequently investigated. Furthermore, a reliability analysis for the desktop computer package is conducted based on the first-passage probability criterion, wherein the product is considered damaged once the response exceeds a predefined threshold.

4.1. Non-Gaussian Excitation Simulation Method and Verification

Non-Gaussian excitation is simulated using the Hermite model, and the simulation is validated through comparison with actual vibration signals.

4.1.1. Simulation Method

A non-Gaussian vibration signal is primarily characterized by its mean μ, variance σ^2, skewness S, and kurtosis K. The

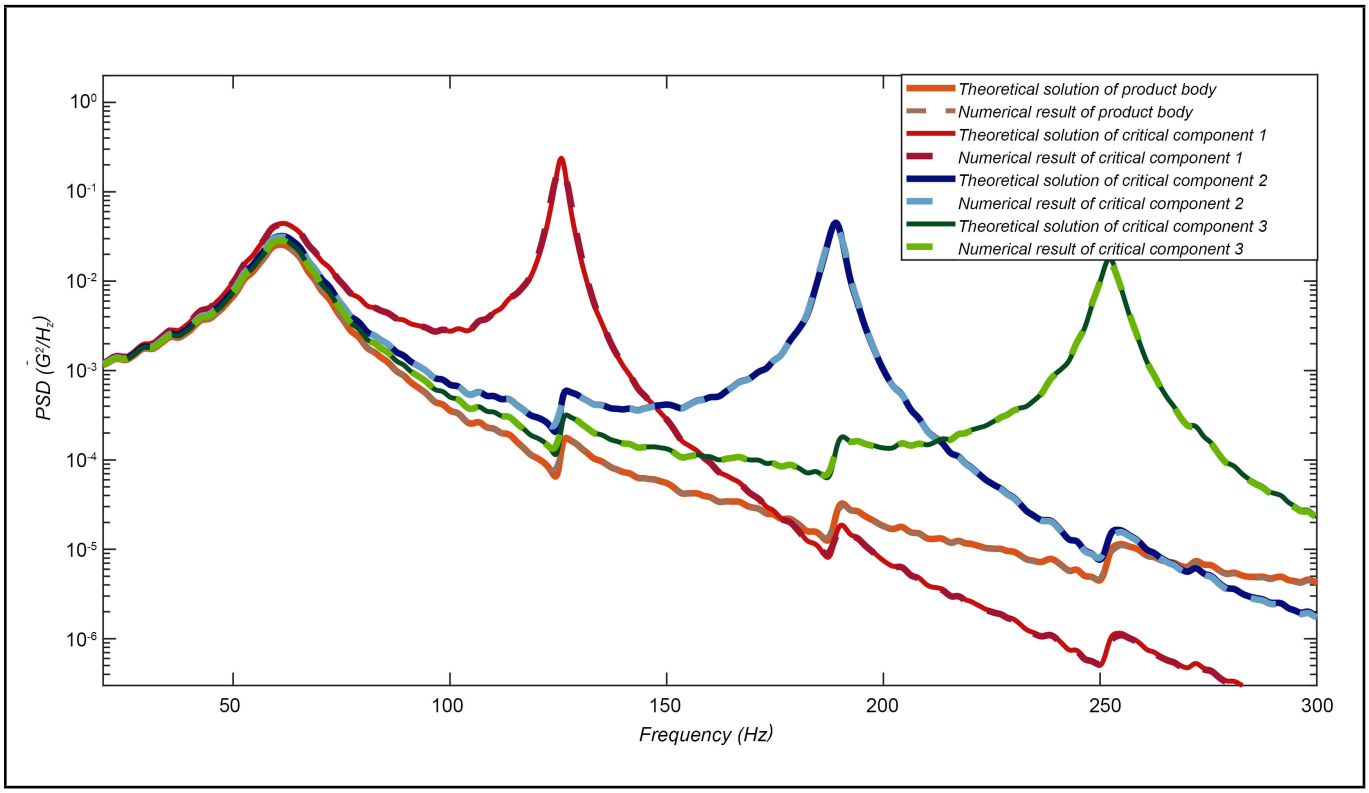

Figure 3. Compare of analytical and numerical solution of the $3+1$ DOF DPPS.

specific calculation formulas for these statistical parameters are given as follows:

$$\begin{cases} \mu = \frac{1}{N}\sum_{i=1}^{N} W_i = m_1; \\ \sigma^2 = \frac{1}{N}\sum_{i=1}^{N}(W_i-\mu)^2 = m_2 - m_1^2; \\ S = \frac{1}{N}\sum_{i=1}^{N}\left(\frac{W_i-\mu}{\sigma}\right)^3 = \frac{m_3}{\sigma^3}; \\ K = \frac{1}{N}\sum_{i=1}^{N}\left(\frac{W_i-\mu}{\sigma}\right)^4 = \frac{m_4}{\sigma^4}; \end{cases} \tag{20}$$

where m_i is the i-order moment of the excitation signal.

According to the Hermite model, a non-Gaussian signal with known mean μ, variance σ^2, skewness S and kurtosis K can be transformed from a Gaussian signal, as expressed below:

$$\ddot{y}_0 = \mu + \sigma\left[\alpha\gamma(t) + h_3(\gamma^2(t)-1) + h_4(\gamma^3(t)-3\gamma(t))\right]; \tag{21}$$

where $\gamma(t)$ represents a standard Gaussian process with zero mean and one variance. α, h_3 and h_4 are determined by the following equations:

$$\begin{cases} \alpha = \dfrac{1}{\sqrt{1+2h_3^2+6h_4^2}}; \\ h_3 = \dfrac{S}{4+2\sqrt{1+1.5(K-3)}}; \\ h_4 = \dfrac{\sqrt{1+1.5\sqrt{K-3}}-1}{18}. \end{cases} \tag{22}$$

In this formula, the parameter α is the scale factor of the non-Gaussian signal $\ddot{y}_0$, while h_3, h_4 are the coefficients of Hermite model, respectively. According to Eqs. (20)–(22), non-Gaussian signals with specific mean μ, variance σ^2, skewness S and kurtosis K can be simulated by Gaussian signals.

4.1.2. Verified by Actual Vibration Signal

Road surface excitations in actual logistics often exhibit pronounced non-Gaussian characteristics. To verify the proposed non-Gaussian signal simulation method, field measurements were conducted on transport vehicles in South China. Sensors recorded random vibration signals, from which the mean μ, variance σ^2, skewness S and kurtosis K are calculated. The resulting values are as follows:

$$\mu = 0.0047,\ \sigma^2 = 0.1191,\ S = 0.0226,\ K = 4.8509. \tag{23}$$

Employing these four statistical parameters along with the aforementioned numerical model, a non-Gaussian random signal possessing identical mean, variance, skewness, and kurtosis is generated via MATLAB programming. The time-domain waveform and probability density distribution histogram of both the simulated and measured signals are presented in Fig. 4 for comparison.

As observed in Fig. 4a, the non-Gaussian vibration signal simulated by the Hermite model-based numerical method closely matches the actual signal in the time domain. Furthermore, Fig. 4b demonstrates excellent agreement between the probability density distributions of the actual and simulated processes, which collectively justifies the equivalence between the deterministic Hermite polynomials and the actual non-Gaussian random excitation. These results indicate that the proposed Hermite polynomial model possesses satisfactory accuracy and feasibility.

4.2. Acceleration Response of the Non-Gaussian Vibration Excited System

Based on the non-Gaussian excitation simulation and the system kinetic equations, a novel approach for analyzing the acceleration response of the system under non-Gaussian vibration excitation is established by integrating the Hermite model with the fourth-order Runge-Kutta algorithm.

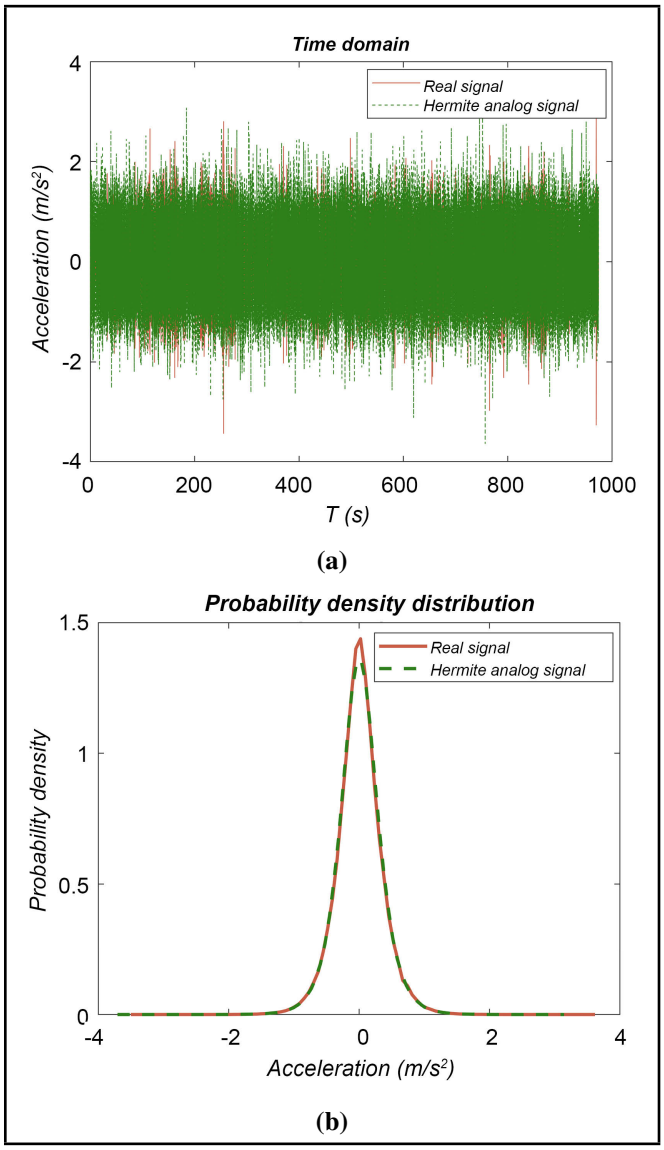

Figure 4. Compare between non-Gaussian real signal and analog signal. (a) Time domain signal process; (b) Probability density distributions.

Table 1. System acceleration response under different excitation kurtosis.

Excitation kurtosis	3	6	9	12	15	21
Kur. of m_p response	2.87	2.93	2.95	3.00	3.08	2.87
Kur. of m_1 response	3.02	3.05	3.02	3.04	3.17	3.02
Kur. of m_2 response	2.60	2.61	2.62	2.67	2.75	2.60
Kur. of m_3 response	2.34	2.35	2.36	2.37	2.40	2.34

Given that kurtosis is a critical parameter for characterizing non-Gaussian signals and is recognized as a key factor in investigating the effect of non-Gaussian excitation on system response, then keeping system paraments as $\omega_p = 63, \omega_1 = 125, \omega_2 = 188, \omega_3 = 251, a_i = 0.01, \xi_p = 0.1, \xi_i = 0.01, \beta = 240$ unchanged, and letting signal paraments takes $L = 0.05,\ \mu = 0, \sigma^2 = 1, S = 0$, the system acceleration response kurtosis for various excitation kurtosis $(3, 6, 9, 15, 18)$ is firstly give in Table 1 and Fig. 5.

It can be observed from Fig. 5 that the kurtosis of the system acceleration response exhibits a distinct nonlinear increase with rising excitation kurtosis. Furthermore, both the kurtosis and root mean square (RMS) values of the acceleration response of critical components are found to be larger than those of the product body.

In Eq. (7), parameter β is the nonlinear characteristic parameter of cushion packaging material, which can measure the degree of material nonlinear strength. In the same way, conducting excitation kurtosis $K = 10$, Fig. 6 depicts the system acceleration response except the difference in nonlinear characteristic parameter β $(60, 120, 240, 480)$.

As observed in Fig. 6, as the nonlinear parameter increases, the resonant frequency of the system response, activated by the cushioning system, decreases monotonically, while the corresponding peak value increases slightly. This behavior exemplifies the "soft spring" nonlinear effect characteristic of hyperbolic tangent packaging systems. Based on this observation, it can be inferred that an optimal nonlinear parameter exists for which the dominant response peaks of the critical components are equalized, thereby minimizing the acceleration response of these components.

4.3. Reliability Analysis for Non-Gaussian Vibration Excited Desktop Computer Package

This section presents a failure analysis of the desktop computer package using the first-passage failure probability of the system acceleration response. First-passage failure occurs when the acceleration response first exceeds the safety threshold, leading to critical component damage and product failure. The first-passage phenomenon is characterized by reliability functions, failure probability, and first-passage rate. Traditional methods include importance sampling[4] and the censored equivalent linearization method.[5] Here, Monte Carlo simulation is adopted to numerically compute the first-passage failure probability of the acceleration response,[6] a method widely applicable and commonly used for nonlinear random vibration problems. The specific procedure is as follows:

First, the total number of samples N_{samp}, time step Δt, time length T and threshold are specified. The discrete time series is then defined as $t_1, t_2 \ldots t_n$, where, $t_i = t_1 + (n-1)\Delta t$.

Second, a non-Gaussian excitation signal is generated and substituted into the equations of motion. The acceleration response is subsequently obtained using the Runge-Kutta method.

Third, the fragility level of the desktop computer is set as the threshold a. For each sample, the first-passage time point is recorded. The first occurrence of threshold crossing is denoted as 1, and all other states as 0, yielding the matrix:

$$\widehat{Y}_{M\times N} = \begin{bmatrix} I_{11} & \ldots & I_{1N} \\ \vdots & \ddots & \vdots \\ I_{M1} & \ldots & I_{MN} \end{bmatrix}; \tag{24}$$

where, $M = N_{samp}$, $N = \frac{T}{\Delta t}$, and:

$$I_{ij} = \begin{cases} 1, & \text{if } \ddot{x}_i(t_j) \gg a, \quad 0 \ll t_j \ll T; \\ 0, & \text{else.} \end{cases} \tag{25}$$

Finally, the first-passage time is evaluated to obtain the failure probability, defined as the number of damaged samples up to a given time point divided by the total number of samples (see Eq. (26)):

$$P\left(t_j\right) = \frac{\sum_{i=1}^{M}\sum_{k=1}^{j} I_{ij}}{M}. \tag{26}$$

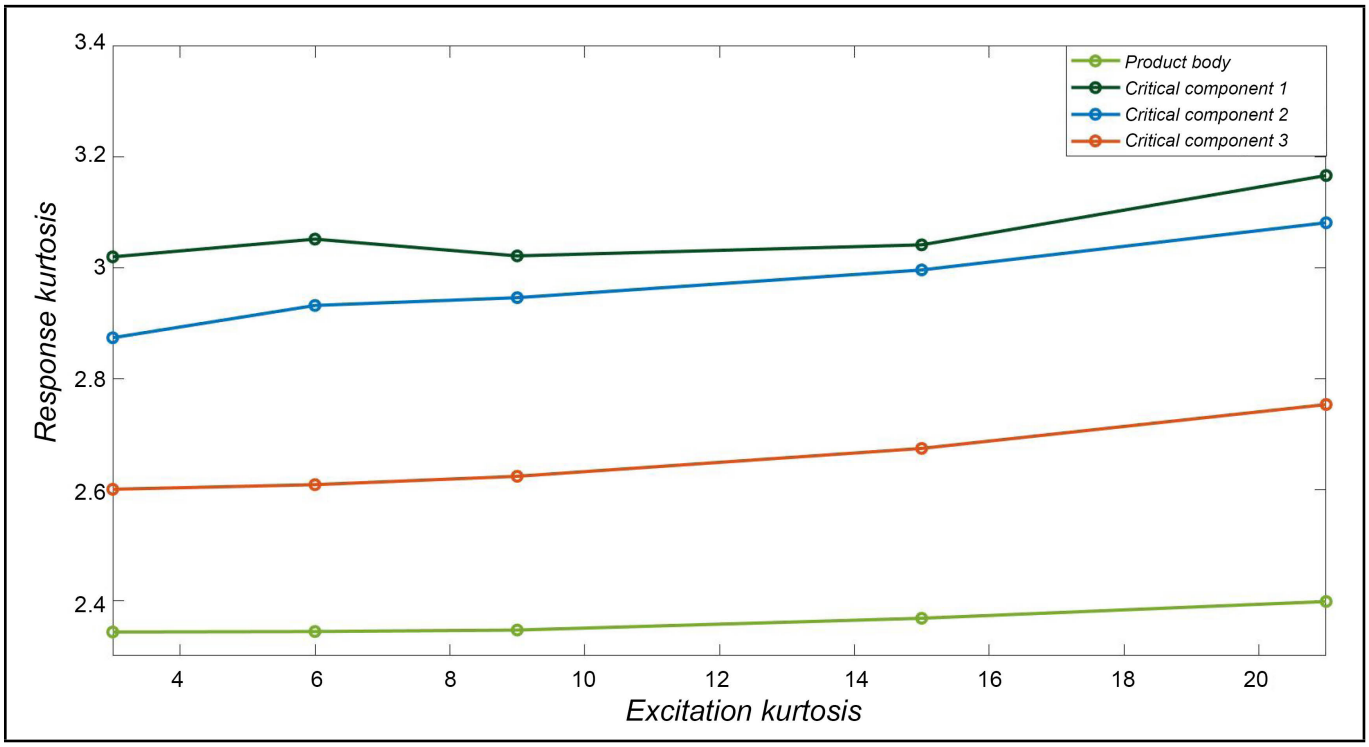

Figure 5. Acceleration response kurtosis under different excitation kurtosis.

Taking the hyperbolic tangent desktop computer package with $3+1$ DOF as an example, assuming that $\omega_p = 63, \omega_1 = 125, \omega_2 = 188$, $\omega_3 = 251$, $a_i = 0.01$, $\xi_p = 0.1$, $\xi_i = 0.01$, $\beta = 240, a = 15\frac{m}{s^2}$, the system acceleration first-passage probability under non-Gaussian signals $\left(L = 0.05, \mu = 0, \sigma^2 = 1, S = 0\right)$ for different excitation kurtosis $(3,\ 6,\ 9,\ 15,\ 21)$ are shown in Fig. 7.

Figure 7 demonstrates that the first-passage probability of the system acceleration response exhibits a nonlinear increase with rising excitation kurtosis, which is attributed to the system nonlinearity. Under identical excitation kurtosis, the first-passage probability of the acceleration response for critical components is substantially higher than that of the product body. Furthermore, the first-passage probability of a critical component decreases as its connected system frequency increases, rendering m_1 the most susceptible to failure and m_3 the least susceptible.

This investigation reveals the failure mechanism of critical components in a desktop computer package subjected to non-Gaussian vibration. The reliability analysis presented above is based on the precondition of a predetermined product fragility, and it readily enables the determination of cushion packaging system parameters for a specified reliability probability. Subsequently, based on these system parameters, an appropriate cushion packaging design can be established for vibration absorption purposes.

5. CONCLUSIONS

This paper presents an approximate analytical solution for efficiently determining the acceleration response spectrum of a hyperbolic tangent MDOF DPPS subjected to Gaussian random vibration. Additionally, a non-Gaussian vibration analysis approach is developed to faithfully reproduce real-world excitations and investigate the system's stochastic acceleration response. The main conclusions are summarized as follows:

First, the proposed approximate analytical solution achieves effective prediction of the acceleration response spectrum under Gaussian excitation, particularly in scenarios involving small displacements and weak nonlinearity.

Second, the established non-Gaussian analysis method can accurately simulate actual non-Gaussian excitations and effectively characterize the non-Gaussian stochastic acceleration response of the system. Elevated non-Gaussian excitation intensity activates the nonlinear effect of parameter β, leading to a reduction in resonant frequency and an increase in response amplitude. Owing to the soft-spring effect exhibited by the hyperbolic tangent cushion, an optimal parameter β^* exists that minimizes the acceleration response of critical components.

Third, the failure mechanism of critical components under non-Gaussian vibration is revealed. On the basis of the predefined product fragility, reliability analysis can be employed to determine the suitable cushion packaging scheme for a target reliability probability.

Future research will concentrate on the design of experimental configurations to further validate the accuracy and effectiveness of the analytical solution proposed in this work.

FUNDING

This work was supported by the Fundamental Research Funds for the Central Universities (Grant No. 21623419).

REFERENCES

[1] Wang, Z. W. *Transport packaging*, China Light Industry Press, Beijing, (2020).

[2] Shires, D. On the time compression (test acceleration) of broadband random vibration tests, *Packag-*

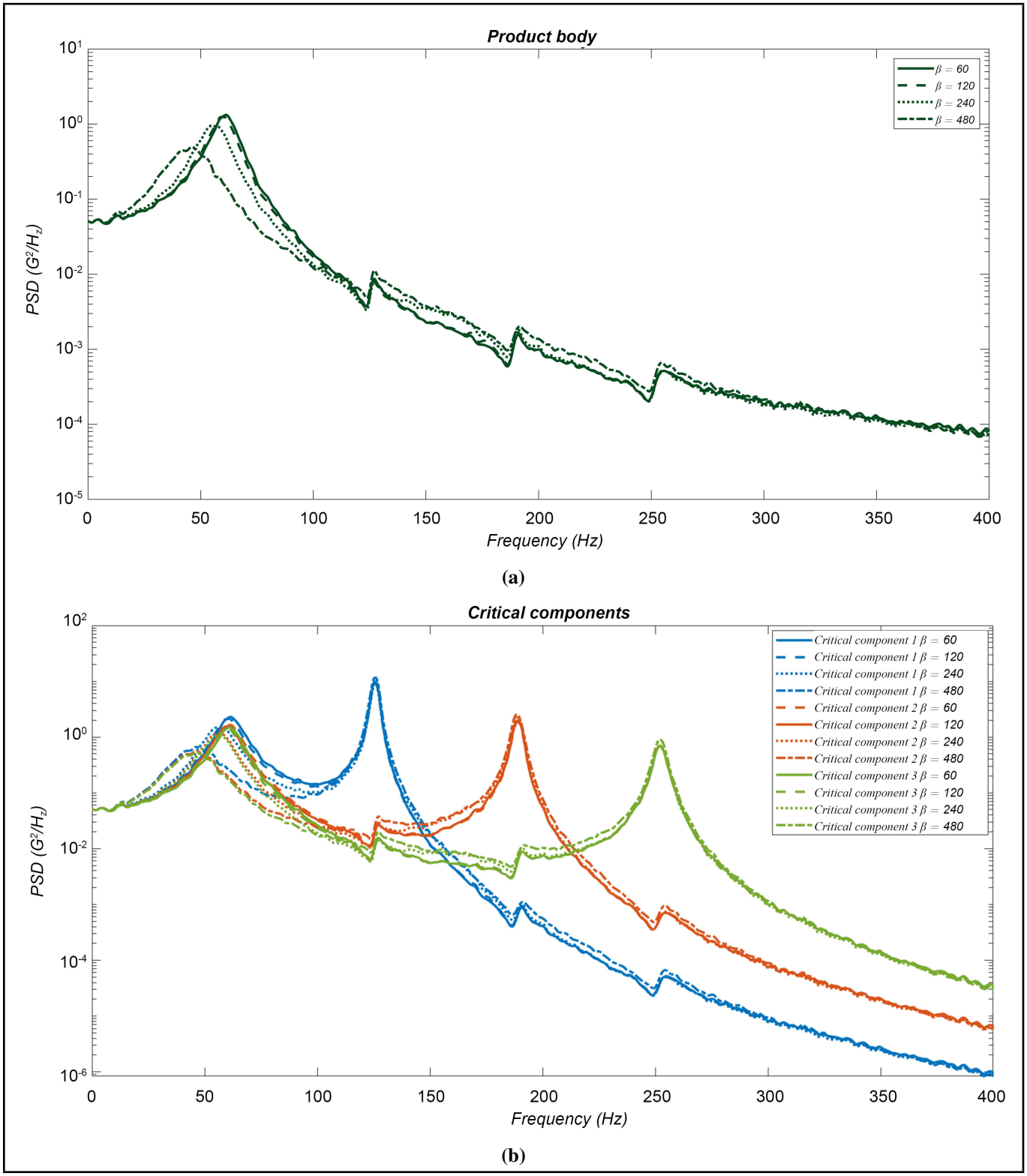

Figure 6. System acceleration response for different nonlinear characteristic parameter. (a) Product body response; (b) Three critical components response.

ing Technology and Science, **24**(2), 75–87, (2011). https://doi.org/10.1002/pts.915

[3] Ge, C. F., Dunno, K., Leinberger, D., et al. Composite analysis of field horizontal long-duration impacts for truck and trailer, *Packaging Technology and Science*, **38**(11), 903–920, (2025). https://doi.org/10.1002/pts.70007

[4] Wang, Z. W. and Wang, L. J. On accelerated random vibration testing of product based on component acceleration RMS-life curve, *Journal of Vibration and Control*, **24**(15), 3384–3399, (2018). https://doi.org/10.1177/1077546317705555

[5] Zhou, H. and Wang, Z. W. Measurement and analysis of vibration levels for express logistics transportation in South China, *Packaging Technology and Science*, **31**(10), 665–678, (2018). https://doi.org/10.1002/pts.2404

[6] Zheng, R. H., Li, J. P., and Chen, H. H. Inves-

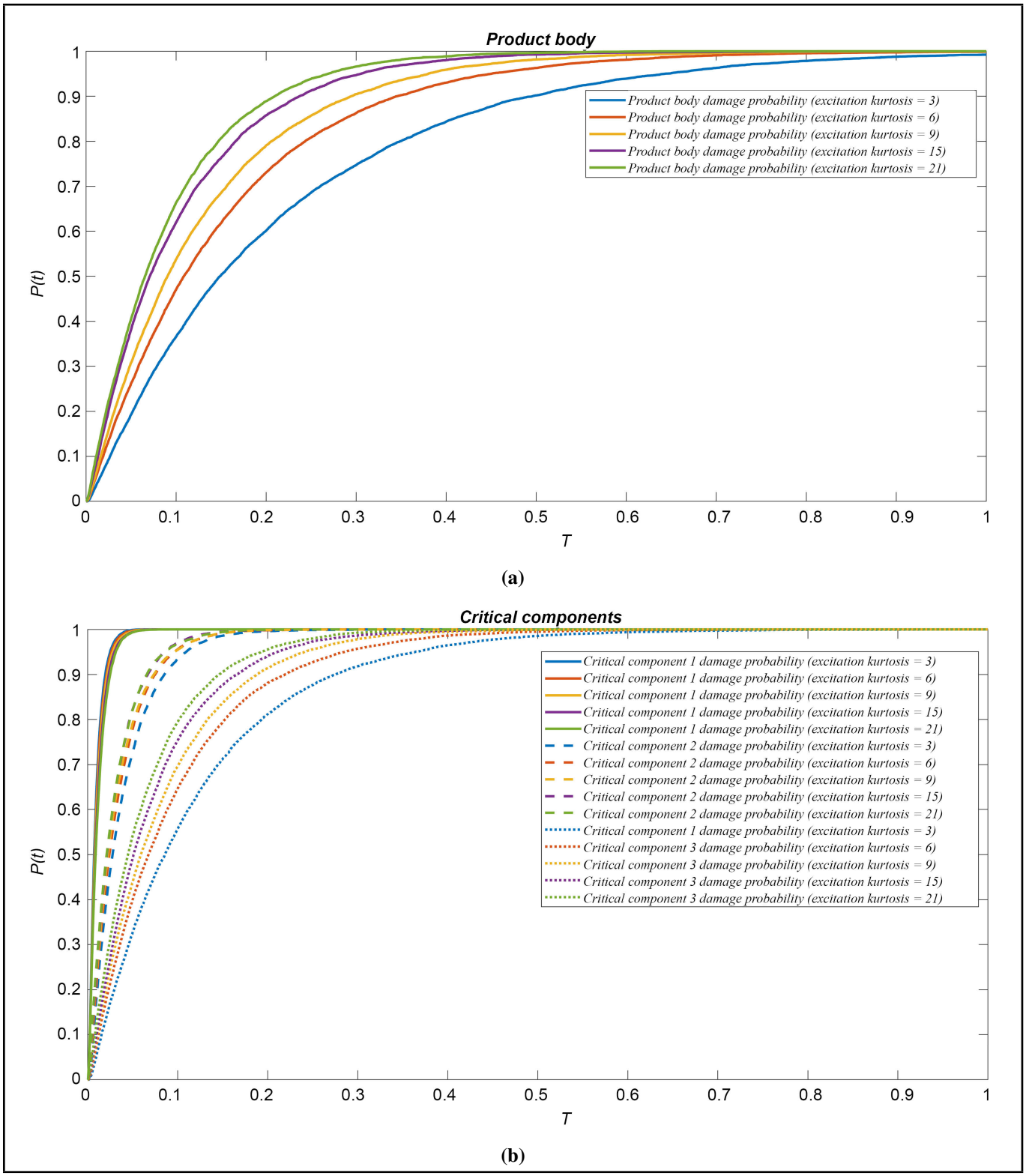

Figure 7. First-passage failure probability of packaged desktop computer for different excitation kurtosis. (a) Product body; (b) Components.

tigation of planar translational and rotational stationary non-Gaussian random vibration test, *Mechanical Systems and Signal Processing*, **191**, 110186, (2023). https://doi.org/10.1016/j.ymssp.2023.110186

[7] Rouillard, V. and Lamb, M. J. Road vehicle shock detection algorithm using the Hilbert envelope, *Computational Methods in Applied Mechanics and Engineering*, **419**, 116637, (2024). https://doi.org/10.1016/j.cma.2023.116637

[8] Singh, J., Singh, S. P., and Joneson, E. Measurement and analysis of US truck vibration for leaf spring and air ride suspensions, and development of tests to simulate these conditions, *Packaging Technology and Science*, **19**(6), 309–323, (2006). https://doi.org/10.1002/pts.732

[9] Lu, F., Ishikawa, Y., Shiina, T., et al. Analysis of shock and vibration in truck transport in Japan, *Packaging Technology and Science*, **21**(8), 479–489, (2008). https://doi.org/10.1002/pts.841

[10] Chonhenchob, V., Singh, S. P., Singh, J. J., et al. Measurement and analysis of truck and rail vibration levels in Thailand, *Packaging Technology and Science*, **23**(2), 91–100, (2010). https://doi.org/10.1002/pts.881

[11] Böröcz, P. and Singh, S. P. Measurement and analysis of vibration levels in rail transport in central Europe, *Packaging Technology and Science*, **30**(8), 361–371, (2017). https://doi.org/10.1002/pts.2225

[12] Kipp, W. I. Random vibration testing of packaged-products: considerations for methodology improvement, *Proc. of 16th IAPRI World Conference on Packaging*, (2008).

[13] Zhou, H. and Wang, Z. W. A new approach for road-vehicle vibration simulation, *Packaging Technology and Science*, **31**(5), 246–260, (2018). https://doi.org/10.1002/pts.2310.

[14] Mindlin, R. D. Dynamics of package cushioning, *Bell System Technical Journal*, **24**(3–4), 353–461, (1945). https://doi.org/10.1002/j.1538-7305.1945.tb00892.x

[15] Kaul, S. Attributes of a vibration isolator design with stiffness nonlinearities, *International Journal of Acoustics and Vibration*, **23**(2), 208–216, (2018). https://doi.org/10.20855/ijav.2018.23.21413

[16] Yang, S. P. and Liu, Z. C. Reliability analysis for product package via probability density function of acceleration random response, *Journal of Vibration and Control*, **30**(7–8), 1841–1854, (2024).

[17] Wang, J., Jiang, J. H., Lu, L. X., et al. Dropping damage evaluation for a tangent nonlinear system with a critical component, *Computers and Mathematics with Applications*, **61**(8), 1979–1982, (2011). https://doi.org/10.1016/j.camwa.2010.08.043

[18] Wang, J., Khan, Y., Lu, L. X., et al. Inner resonance of a coupled hyperbolic tangent nonlinear oscillator arising in a packaging system, *Journal of Applied Mathematics and Computing*, **218**(5), 7876–7879, (2012). https://doi.org/10.1016/j.amc.2012.02.005

[19] Yang, S. P. and Wang, Z. W. Dynamic response of asymmetric and nonlinear packaging system under random excitation, *Shock and Vibration*, **2020**(1), 1–17, (2020). https://doi.org/10.1155/2020/8840147

[20] Newton, R. E. Fragility assessment theory and test procedure, Monterey Research Laboratory Inc, (1968).

[21] Wang, Z. L., Wu, C. F., and Xi, D. C. Damage boundary of a packaging system under rectangular pulse excitation, *Packaging Technology and Science*, **11**(4), 189–202, (1998). https://doi.org/10.1002/(SICI)1099-1522(199807/08)11:4<189::AID-PTS430>3.0.CO;2-7

[22] Wang, Z. W. Shock spectra and damage boundary curves for hyperbolic tangent cushioning system and their important features, *Packaging Technology and Science*, **14**(4), 149–157, (2001). https://doi.org/10.1002/pts.544

[23] Wang, J., Duan, F., Jiang, J. H., et al. Dropping damage evaluation for a hyperbolic tangent cushioning system with a critical component, *Journal of Vibration and Control*, **18**(10), 1417–1421, (2012). https://doi.org/10.1177/1077546311421515

[24] Jiang, J. H. and Wang, Z. W. Dropping Damage Boundary Curves for Cubic and Hyperbolic Tangent Packaging Systems Based on Key Component, *Packaging Technology and Science*, **25**(7), 397–411, (2012). https://doi.org/10.1002/pts.985

[25] Rouillard, V. and Sek, M. A. Monitoring and simulating non-stationary vibrations for package optimization, *Packaging Technology and Science*, **13**(4), 149–156, (2000). https://doi.org/10.1002/1099-1522(200007)13:4<149::AID-PTS508>3.0.CO;2-A

[26] Thakur, K. P. and Pang, D. Simulating complex loading patterns in the stack of packages, *Proc. of the 10th IAPRI World Conference on Packaging*, (1997).

[27] Gan, C. B. Stochastic averaging of packaging oscillatory system under stochastic excitation, *Package Engineering*, **26**(5), 18–20, (2005).

[28] Zhu, D. P. Vibration reliability analysis for critical component of nonlinear package system, *Journal of Vibration and Shock*, **38**(18), 109–114, (2019).

[29] Zhu, D. P. Time-dependent reliability analysis of package under non-Gaussian excitation, *Journal of Vibration and Shock*, **39**(16), 96–102, (2020).

[30] Zhang, R. L., Shen, Y. J., and Yang, X. T. Dynamic analysis of asymmetric piecewise linear systems, *Applied Mathematics and Mechanics*, **46**(4), 633–646, (2025). https://doi.org/10.1007/s10483-025-3234-9

[31] Wang, Q. Y., Cheng, J. N., Zhao, Z. L., et al. Dynamics analysis of cold rolling system under multi-piecewise nonlinear constraint coupled with dynamic rolling force, *Journal of the Brazilian Society of Mechanical Sciences and Engineering*, **47**(10), 489, (2025).

[32] Song, H. Y. A modification of homotopy perturbation method for a hyperbolic tangent oscillator arising in nonlinear packaging system, *Journal of Low Frequency Noise, Vibration & Active Control*, **38**(3-4), 914–917, (2019). https://doi.org/10.1177/1461348418822135

[33] Yang, S. P. and Wang, Z. W. Acceleration spectrum analysis of hyperbolic tangent package under random excitation, *Packaging Technology and Science*, **34**(9), 579–587, (2021). https://doi.org/10.1002/pts.2596

[34] Yang, S. P., Su, R. Q., Wang, Z. W., et al. A new approach for non-Gaussian vibration analysis of hyperbolic tangent package with a critical component, *Mathematical Methods in the Applied Sciences*, **47**(5), 3596–3613, (2024). https://doi.org/10.1002/mma.8883

[35] Wang, Z. W. and Wang, L. J. Accelerated random vibration testing of transport packaging system based on acceleration PSD, *Packaging Technology and Science*, **30**(10), 621–643, (2017). https://doi.org/10.1002/pts.2306

[36] Clark, A. J. Multiple passive tuned mass damper for reducing earthquake induced building motion, *Proc. of the 9th World Conference on Earthquake Engineering*, **5**, 779–784, (1998).

[37] Ormondroyd, J. and Den Hartog, J. P. The theory of the dynamic vibration absorber, *Transactions of the American society of Mechanical Engineers*, **49**(2), 021007, (1928). https://doi.org/10.1115/1.4058553

[38] Crandall, S. H. and Mark, W. D. *Random Vibration in Mechanical Systems*, Academic Press, (1963).

[39] Zuo, L. and Nayfeh, S. A. Optimization of the individual stiffness and damping parameters in multiple-tuned-mass-damper systems, *Journal of Vibration and Acoustics*, **127**(1), 77–83, (2005). https://doi.org/10.1115/1.1855929

[40] Wong, K. K. and Johnson, J. Seismic energy dissipation of inelastic structures with multiple tuned mass dampers, *Journal of Engineering Mechanics*, **135**(4), 265–275, (2009). https://doi.org/10.1061/(ASCE)0733-9399(2009)135:4(265)

[41] Gatti, G. Fundamental insight on the performance of a nonlinear tuned mass damper, *Meccanica*, **53**(1), 111–123, (2018). https://doi.org/10.1007/S11012-017-0723-0

[42] Wu, P. H., Xiao, J., and Zhao, Y. Power spectrum analysis and optimization design of nonlinear energy sink under random excitation, *Journal of Vibration Engineering & Technologies*, **12**(4), 5663–5673, (2024). https://doi.org/10.1007/s42417-023-01210-1

[43] Gendelman, O. V., Starosvetsky, Y. and Feldman, M. Attractors of harmonically forced linear oscillator with attached nonlinear energy sink I: description of response regimes, *Nonlinear Dynamics*, **51**(1), 31–46, (2008). https://doi.org/10.1007/s11071-006-9167-0

[44] Habib, G., Detroux, T., Viguié, R., et al. Nonlinear generalization of Den Hartog's equal-peak method, *Mechanical Systems and Signal Processing*, **52**, 17–28, (2015). https://doi.org/10.1016/j.ymssp.2014.08.009

[45] Picavea, J., Gameros, A., Yang, J., et al. Vibration suppression using tuneable flexures acting as vibration absorbers, *International Journal of Mechanical Sciences*, **222**, 107238, (2022). https://doi.org/10.1016/j.ijmecsci.2022.107238

[46] Huu, T. P., Miura, N., and Iba, D. Multi active tuned mass dampers for earthquake-induced vibration response control of high rise building, *Journal of Mechanical Science and Technology*, **36**(4), 1655–1666, (2022). https://doi.org/10.1007/s12206-022-0304-6

[47] Long, Z., Shen, W., and Zhu, H. On energy dissipation or harvesting of tuned viscous mass dampers for SDOF structures under seismic excitations, *Mechanical Systems and Signal Processing*, **189**, 110087, (2023). https://doi.org/10.1016/j.ymssp.2022.110087

[48] Bermany, T. H. R., Osman, S. A., and Yatim, M. Y. M. A state-of-the-art analysis of base isolation systems and future directions for developing a novel multi-directional smart-hybrid isolation system integrated with earthquake early warning system for building structures, *Results in Engineering*, **25**, 104501, (2025). https://doi.org/10.1016/j.rineng.2025.104501

[49] Batou, A. and Adhikari, S. Optimal parameters of viscoelastic tuned-mass dampers, *Journal of Sound and Vibration*, **445**, 17–28, (2019). https://doi.org/10.1016/j.jsv.2019.01.010

[50] Argenziano, M., Faiella, D., Carotenuto, A. R., et al. Generalization of the Den Hartog model and rule-of-thumb formulas for optimal tuned mass dampers, *Journal of Sound and Vibration*, **538**, 117213, (2022). https://doi.org/10.1016/j.jsv.2022.117213

[51] Zhang, Y., Kong, X., and Yue, C. Vibration analysis of a new nonlinear energy sink under impulsive load and harmonic excitation, *Communications in Nonlinear Science and Numerical Simulation*, **116**, 106837, (2023). https://doi.org/10.1016/j.cnsns.2022.106837

[52] Saeed, A. S., Abdul, N. R., and AL-Shudeifat, M. A. A review on nonlinear energy sinks: designs, analysis and applications of impact and rotary types, *Nonlinear Dynamics*, **111**(1), 1–37, (2023).

[53] Ge, C., Xu, Z., Du, K., et al. An improved inverse power law model for accelerated fatigue life prediction of 6061-T6 and AZ31B-F, *Engineering Failure Analysis*, **138**, 106381, (2022). https://doi.org/10.1016/j.engfailanal.2022.106381

[54] Géhin, A., Bégin-Drolet, A., and Lépine, J. Method for measuring friction performance for tertiary packaging under dynamic loading representative of transport conditions, *Packaging Technology and Science*, **38**(12), 979–985, (2025). https://doi.org/10.1002/pts.70012

[55] Zhou, H. and Wang, Z. W. Comparison study on simulation effect of improved simulation methods for packaging random vibration test, *Packaging Technology and Science*, **32**(3), 119–131, (2019). https://doi.org/10.1002/pts.2421

[56] Nakai, D. Generating random vibration targeting acceleration kurtosis and probability distribution by combining gaussian vibrations, *Packaging Technology and Science*, **39**(4), 395–404, (2025). https://doi.org/10.1002/pts.70036

[57] Fernando, I., Fei, J., Stanley, R., et al. Developing an accelerated vibration simulation test for packaged bananas, *Postharvest Biology and Technology*, **173**, 111400, (2021). https://doi.org/10.1016/j.postharvbio.2020.111400

[58] Socha, L. and Soong, T. T. Linearization in analysis of nonlinear stochastic systems, *Applied Mechanics Reviews*, **44**, 399–422, (1991). https://doi.org/10.1115/1.3119486

[59] Ito, K. *On stochastic differential equations*, American Mathematical Soc, (1951).

[60] Clough, R. Effect of stiffness degradation on earthquake ductility requirements, *Proc. of Japan Earthquake Engineering Symposium*, (1966).

[61] Deng, M. L., Fu, Y., and Huang, Z. L. Asymptotic analytical solutions of first-passage rate to quasi-nonintegrable Hamiltonian systems, *ASME Journal of Applied Mechanics*, **81**(8), 081012, (2014). https://doi.org/10.1115/1.4027706